Journal of The Electrochemical Society, **157** (3) H377-H380 (2010)
0013-4651/2010/157(3)/H377/4/$28.00 © The Electrochemical Society

Crystal Quality of 3C-SiC Influenced by the Diffusion Step in the Modified Four-Step Method

Wei-Yu Chen,[a] Wei-Lin Wang,[c] Jui-Min Liu,[a] Chien-Cheng Chen,[a] Jenn-Chang Hwang,[a,z] Chih-Fang Huang,[b] and Li Chang[c]

[a]*Department of Materials Science and Engineering and* [b]*Department of Electrical Engineering, National Tsing Hua University, Hsinchu City 30013, Taiwan*
[c]*Department of Materials Science and Engineering, National Chiao Tung University, Hsinchu City 30013, Taiwan*

The atomic arrangement and bonding characteristics of void-free 3C-SiC/Si(100) grown by the modified four-step method are presented. Without the diffusion step, Si–C bonds are partially formed in the as-carburized layer on Si(100). The ratio of C–C bonds to Si–C bonds is about 7:3, which can be lowered to about 1:9 after the diffusion step at 1350°C for 5 min or at 1300°C for 7 min according to C 1s core level spectra. The residual C–C bonds cannot be removed, which is associated with an irregular atomic arrangement (amorphous) located either at the 3C-SiC/Si(100) interface or at the intersection of twin boundaries in the 3C-SiC buffer layer based on the lattice image taken by transmission electron microscope. The diffusion step helps the formation of Si–C bonds more completely and results in a SiC buffer layer of high quality formed on Si(100) before the growth step. However, twins and stacking faults still appear in the 3C-SiC buffer layer after the diffusion step. The formation mechanism of the 3C-SiC buffer layer is proposed and discussed.
© 2010 The Electrochemical Society. [DOI: 10.1149/1.3294700] All rights reserved.

Manuscript submitted September 11, 2009; revised manuscript received December 11, 2009. Published February 4, 2010.

Silicon carbide (SiC) is a wide bandgap semiconductor for high power and high frequency devices due to its excellent thermal and electrical characteristics.[1,2] Single-crystalline SiC in 4H and 6H polytypes is expensive and commercially available for device fabrication.[3,4] As a means to lower the production cost, the heteroepitaxy of 3C-SiC on Si has attracted attention in the past decades. The difficulty to grow a 3C-SiC layer of good quality on Si arises from large lattice mismatch ($\sim$20%) and difference in thermal expansion coefficients ($\sim$8%). The breakthrough in the growth of 3C-SiC on Si using a buffer layer was first reported by Nishino et al.[5] A conventional three-step method, consisting of cleaning, carburization, and growth, was proposed and illustrated.[5] The carburization step plays two roles in the growth of 3C-SiC on Si in the conventional three-step method. One is to supply carbon atoms in the form of amorphous carbon onto Si at carburization temperature, usually at 1250°C for the $C_3H_8/H_2/SiH_4$ system. The other is to form a 3C-SiC buffer layer by driving Si atoms out of the Si substrate into the amorphous carbon layer at carburization temperature. The carburization step has become a standard procedure for the growth of 3C-SiC on Si since then.[6-11] However, voids[6-9,12-16] and micropipes,[17,18] which are attributed to the out-diffusion of Si atoms, appear at the 3C-SiC/Si interface after carburization. In addition to voids and micropipes, planar defects such as twins and stacking faults are generated in the 3C-SiC buffer layer as a result of the strain relaxation at the lattice-mismatched SiC/Si interface. The planar defects are generated and propagated along the {111} planes in 3C-SiC grown on Si, which usually occurs at a high heating rate and a low partial gas pressure of carbon, reported by Cimalla et al. and Yun et al.[19,20]

The conventional three-step method is a long time process because it requires cooling the samples back to room temperature between each step. It takes about 1 h to cool the sample from process temperature to room temperature in each step. The conventional three-step method can be performed either by atmospheric pressure chemical vapor deposition (APCVD) or by low pressure chemical vapor deposition (LPCVD). Zorman et al. showed in 1995 that the void-free growth of 3C-SiC films on a large area of Si substrates was achieved by APCVD using the conventional three-step process.[21] However, two major issues associated with the LPCVD growth of 3C-SiC epitaxial films using the conventional three-step method remain to be solved. One is the voids at the SiC/Si interface because the out-diffusion of Si atoms is severe in LPCVD. The other is the planar defects (twins and stacking faults) generated in the 3C-SiC buffer layer due to the lattice-mismatch-induced stress at the SiC/Si interface.

In 2008, Chen et al. developed the modified four-step method (cleaning, carburization, diffusion, and growth) associated with the LPCVD growth by inserting a diffusion step and by removing the cooling step in the conventional three-step method.[22] The modified four-step method can be performed in a shorter time than the conventional three-step method because the cooling process between each step is removed. A void-free 3C-SiC film of high quality can be grown on Si(100) in a mixed gas of SiH_4–C_3H_8–H_2 using LPCVD. The quality of the 3C-SiC buffer layer is improved by introducing the diffusion step in the modified four-step method reported in our previous work.[22] The major role of the diffusion step is to assist the Si–C bond formation more efficiently by decoupling the out-diffusion of Si atoms from the deposition of amorphous carbon. However, the atomic arrangement and bonding characteristics of the 3C-SiC buffer layer are unclear.

In this paper, we present the variation in structural and bonding characteristics of the 3C-SiC buffer layer grown on Si(100) by LPCVD at different diffusion temperatures and times. The formation mechanism of the 3C-SiC buffer layer is also proposed to explain the growth of high quality 3C-SiC on Si(100) by the modified four-step method according to the structural and bonding information.

Experimental

A horizontal cold-wall-type LPCVD system with induction heating was used for the growth of 3C-SiC on a p-type Si(100) substrate, which was illustrated previously by other groups.[23] The Si(100) substrate of 1×1 cm was dipped in 1% HF for 30 s, rinsed by deionized water, and then placed on a SiC-coated graphite susceptor that was heated by radio-frequency induction. The mixed gas of SiH_4 (5% in H_2) and C_3H_8 (4N) was carried by H_2 (5N) into the LPCVD chamber for the growth of 3C-SiC on Si(100). The temperature was ramped up at a rate of about 11°C/s and measured by a thermocouple and an IR pyrometer. The total pressure was varied by controlling the throttle valve between the LPCVD chamber and the mechanical pump. Most samples were treated with the modified four-step method shown in Fig. 1a. Some samples were treated with the modified four-step method without the growth step shown in Fig. 1b for comparison.

The optimum experimental parameters for the modified four-step method listed in Table I were reported in our previous work.[22] The growth rate of 3C-SiC was approximately 3 μm/h, and all the 3C-

[z] E-mail: jch@mx.nthu.edu.tw

Downloaded on 2014-04-24 to IP 140.113.38.11 address. Redistribution subject to ECS terms of use (see ecsdl.org/site/terms_use) unless CC License in place (see abstract).

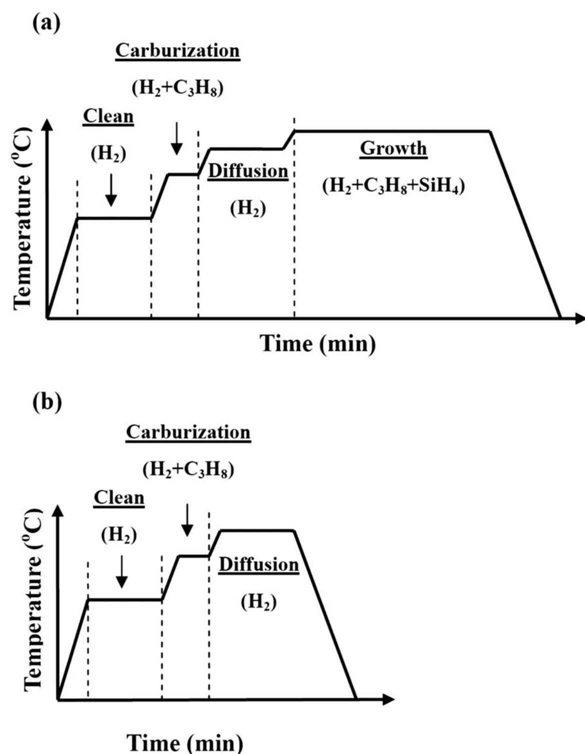

Figure 1. Schematic showing the processes for the growth of 3C-SiC on Si. (a) The modified four-step method. (b) The modified four-step method without the growth step.

SiC film thicknesses were kept at 1.5 μm in this study. The structural information of 3C-SiC films was characterized using a Rigaku D/MAX2000 X-ray diffractometer (XRD) with a Cu Kα radiation (1.5405 Å) and an FEI TECNAI G2 transmission electron microscope (TEM). The bonding characteristics of 3C-SiC films were characterized using X-ray photoelectron spectroscopy (XPS, PHI ESCA 1600).

Results and Discussion

The crystal qualities of 3C-SiC films grown on Si(100) using the modified four-step method are strongly affected by temperature and process time at the diffusion step, as shown in the XRD spectra in Fig. 2a and b. Only the (200) peak of 3C-SiC appears in each XRD spectrum, indicating that the as-grown 3C-SiC film is either highly oriented or epitaxial. The (200) peak of 3C-SiC increases in intensity with process time at 1300°C, as shown in Fig. 2a. The role of the diffusion step at 1300°C is to assist the growth of 3C-SiC films of good quality before the growth step. When the temperature is raised from 1300 to 1350°C, a higher intensity of 3C-SiC(200) can be achieved at a shorter process time. The improvement of the crystal qualities of the 3C-SiC films by the diffusion step is also confirmed by X-ray rocking curve measurements. The full width at half-maximum (fwhm) of 3C-SiC(200) reduces from 0.77 to 0.73

Table I. Optimal experimental parameters at each step in the modified four-step method.

	Clean	Carburization	Diffusion	Growth
H_2 (sccm)	1000	1000	1000	1000
C_3H_8 (sccm)	0	10	0	3
SiH_4 (sccm)	0	0	0	20
Temperature (°C)	900	1250	1350	1420
Pressure (Torr)	10	2	2	0.8

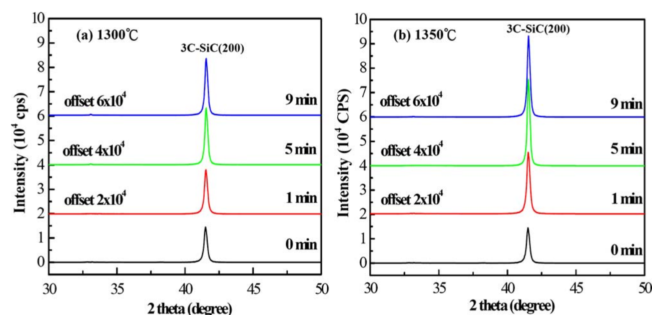

Figure 2. (Color online) XRD spectra of the 3C-SiC films grown on Si(100) by the modified four-step method at different diffusion conditions: (a) 1300 and (b) 1350°C.

and from 0.77 to 0.67 by treating samples with the diffusion step at 1300 and 1350°C for 9 min, respectively, as listed in Table II. A better crystal quality of the 3C-SiC film can be obtained within a shorter process time at a higher temperature.

The quality improvement of the SiC buffer layer is further investigated by XPS and TEM for the as-diffused 3C-SiC/Si(100) samples (grown by the modified four-step method without the growth step in our LPCVD system). The Si–C bond formation of the as-diffused 3C-SiC/Si(100) samples is clearly illustrated by the curve-fit of the C 1s core level spectra in Fig. 3a and b. All the Si(100) samples are carburized at a C_3H_8 partial pressure of 1.9 $\times 10^{-2}$ Torr and at 1250°C for 1.5 min before treating with the diffusion step at 1300 or 1350°C. There exists a broad shoulder (or peak) on the left side of the prominent C 1s peak at ~283 eV, indicating the existence of two types of carbon bonding environments in the 3C-SiC buffer layer after diffusion. The two C 1s components located at 284.5 and 283.2 eV are required to obtain consistent curve-fit results, which are assigned as C–C and Si–C bonds, respectively. The difference in the C 1s binding energies of the C–C and Si–C bonds results from the different amounts of charge transfer. The corresponding curve-fit results are also listed in Table II. The ratio of Si–C bonds to C–C bonds for the as-carburized 3C-SiC/Si(100) sample is about 3:7, suggesting that Si–C bonds form partially at the carburization step. In other words, the Si atoms diffused out of Si(100) are not enough to transform the as-carburized layer into SiC and result in excess carbon (C–C bonds) that resided in the as-carburized Si(100) layer. The excess carbon

Table II. FWHM of the SiC(200) peak and the area percentages of the C–C and C–Si bonds deconvoluted from C 1s core level spectra taken from the samples treated with different diffusion conditions (temperature and process time).

Diffusion temperature (°C)	Diffusion time (min)	fwhm (°)	C–C (%)	C–Si (%)
1300	0	0.77	69[a]	31[a]
	1	0.76	48	52
	3	—	27	73
	5	0.74	19	81
	7	—	8	92
	9	0.73	8	92
1350	0	0.77	69[a]	31[a]
	1	0.71	36	64
	3	—	19	81
	5	0.67	10	90
	7	—	8	92
	9	0.67	7	93

[a] Data extracted from the C 1s core level spectra for the sample without the diffusion treatment.[22]

Downloaded on 2014-04-24 to IP 140.113.38.11 address. Redistribution subject to ECS terms of use (see ecsdl.org/site/terms_use) unless CC License in place (see abstract).

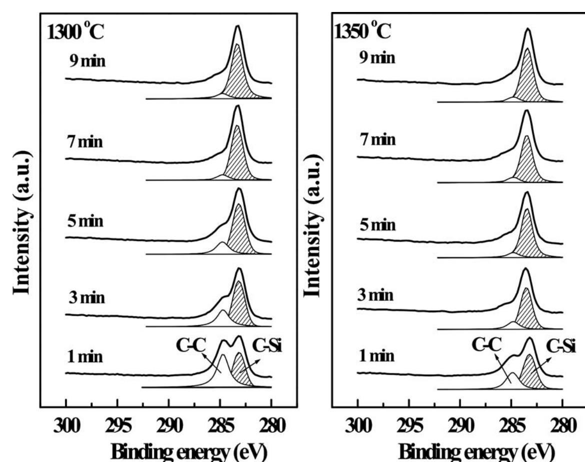

Figure 3. C 1s core level spectra of the as-diffused 3C-SiC/Si(100) samples as a function of temperature and process time: (a) 1300 and (b) 1350°C. The curve-fit results are marked with C–C and C–Si to represent their corresponding bonding components.

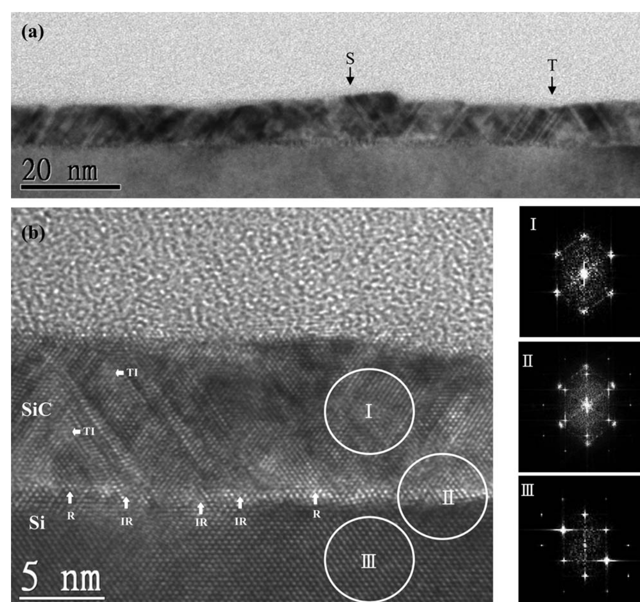

Figure 4. Cross-sectional view TEM micrographs taken at the SiC/Si(100) interface. (a) Bright-field TEM image. (b) HRTEM lattice image. Three different regions (I, II, and III) are circled to obtain the FFT images (equivalent to ED patterns).

results from the carbon deposition at a high C_3H_8 flow rate (10 sccm) that is designed to cover the Si(100) surface quickly to avoid the interfacial void formation at the carburization step. The as-carburized Si(100) surface with excess carbon can be further transformed into a SiC buffer layer at the diffusion step before the growth step. After diffusion at 1300°C, the amount of Si–C bonds increases with process time and reaches a maximum value at approximately 7 min, accompanied with the reduction in C–C bonds. The highest ratio of Si–C bonds to C–C bonds is about 9:1. The ~10% excess carbon (C–C bonds) still resides in the SiC buffer layer, which is probably located at the intersection of twins that are illustrated in TEM micrographs and discussed later. A similar result occurs at a faster rate for the diffusion step at 1350°C. The relative amount of Si–C bonds increases with process time and reaches a maximum value at approximately 5 min, as indicated in Table II. The faster increase rate of Si–C bonds at 1350°C indicates that the Si–C bond formation in the SiC buffer layer is controlled by a diffusion-limited process. The Si–C bond formation in the SiC buffer layer enables the growth of a SiC film of better quality at the growth step, supported by the higher intensity of 3C-SiC(200) shown in Fig. 2a and b and by the smaller fwhm of the corresponding XRD rocking curve listed in Table II.

The structural information of the SiC buffer layer is further characterized by using high resolution transmission electron microscopy (HRTEM). Figure 4a shows the bright-field cross-sectional TEM micrograph of the as-diffused sample treated at 1350°C for 9 min. An ultrathin SiC layer of ~10 nm thick is stacked on Si(100) with a surface roughness of less than 1 nm. Several twins and stacking faults are identified and marked with "T" and "S," respectively. The atomic arrangement at the 3C-SiC/Si(100) interface is revealed in the HRTEM lattice image in Fig. 4b. Many planar defects, including twins and stack faults, are inclined on {111} planes of 3C-SiC near the 3C-SiC/Si(100) interface. The generation of twins and stacking faults is attributed to high heating rate and low C_3H_8 partial pressure, according to previous publications.[19,20] The propagation of twins stops when two inclined twins intersect, reported by Yagi and Nagasawa.[24] The atomic arrangement at the intersection of twins, marked with "TI," is irregular (amorphous) in the lattice image in Fig. 4b. The excess carbon (C–C bonds) is probably located at the TI locations. The ⟨111⟩ directions in the lattice image of the 3C-SiC buffer layer in Fig. 4b are not straight, indicating that the 3C-SiC crystal is distorted due to the lattice-mismatch-induced stress at the 3C-SiC/Si(100) interface. Moreover, the ~0.7 nm thick interface is not uniform, which is blended with regular (R) and irregular atomic arrangements. The excess carbon (C–C bonds) is probably located at the irregular locations. Three fast Fourier transform (FFT) images, taken from three small regions circled in the lattice image (I, II, and III), are placed in Fig. 4b, next to the HRTEM lattice image. The FFT image I with clear spots is identified to be the electron diffraction (ED) pattern of 3C-SiC looking from the zone axis [110], indicating the good crystalline quality of 3C-SiC. The FFT image II, taken from the interface, is identified to be a combination of Si and 3C-SiC ED patterns. Both Si and 3C-SiC are in an epitaxial orientation relationship. The FFT image III with sharp spots is determined to be the ED pattern of Si. The three FFT images and the lattice image in Fig. 4b support that the ultrathin SiC buffer layer is single crystalline. However, some planar defects and irregular atomic arrangements exist in the 3C-SiC buffer layer.

The formation of the SiC buffer layer at carburization and diffusion steps is proposed and described as follows: First, the amorphous carbon is deposited on Si(100) and partially reacted with Si atoms to form Si–C bonds when a high flow rate (10 sccm) of C_3H_8 is introduced into the LPCVD chamber at the carburization step. The ratio of C–C bonds to Si–C bonds is about 7:3, right after the carburization step, according to the XPS data. There should be a SiC nuclei dispersed in a matrix of amorphous carbon after the carburization step because the volume ratio of C–C bonds is very large (~70%). Second, the diffusion step assists in the Si–C bond formation more completely. The TEM image indicates that the SiC layer is finally in a crystal form on Si(100) after the diffusion step. This supports the fact that SiC nuclei grow in size by forming Si–C bonds via the out-diffusion of Si atoms toward the amorphous carbon layer. The out-diffusion of Si atoms stops, and the ratio of the C–C bonds to the Si–C bonds reaches ~1:9 after the diffusion step. A continuous SiC buffer layer is finally formed on Si(100). The residual C–C bonds are probably associated with irregular atomic arrangements, which are located either at the 3C-SiC/Si(100) interface or at the intersection of twin boundaries shown in the TEM lattice image in Fig. 4b.

Conclusions

A void-free 3C-SiC/Si(100) interface can be achieved by LPCVD using the modified four-step method. The formation of Si–C bonds is not sufficient at the carburization step. The 3C-SiC nuclei are dispersed in a matrix of amorphous carbon after the car-

Downloaded on 2014-04-24 to IP 140.113.38.11 address. Redistribution subject to ECS terms of use (see ecsdl.org/site/terms_use) unless CC License in place (see abstract).

burization step. The diffusion step helps the formation of Si–C bonds more completely before the growth of 3C-SiC. A 3C-SiC buffer layer of high quality is formed on Si(100) after the diffusion step. However, twins and stacking faults, resulting from the relaxation of strain, cannot be removed after the diffusion step.

Acknowledgment

The work is sponsored by the National Science Council through the project NSC96-2218-E-007-003.

National Tsing Hua University assisted in meeting the publication costs of this article.

References

1. C. M. Zettetling, *Process Technology for Silicon Carbide Device*, p. 4, Institution of Electrical Engineers, London (2002).
2. J. B. Casady and R. W. Johnson, *Solid-State Electron.*, **39**, 1409 (1996).
3. J. W. Palmour, J. A. Edmonda, H. S. Konga, and C. H. Carter, *Physica B*, **185**, 461 (1993).
4. C. E. Weitzel, J. W. Palmour, C. H. Carter, K. Moore, K. J. Nordquist, S. Allen, C. Thero, and M. Bhatnagar, *IEEE Trans. Electron Devices*, **43**, 1732 (1996).
5. S. Nishino, J. A. Powell, and H. A. Hill, *Appl. Phys. Lett.*, **42**, 460 (1983).
6. A. J. Steckl and J. P. Li, *IEEE Trans. Electron Devices*, **39**, 64 (1992).
7. P. Liaw and R. F. Davis, *J. Electrochem. Soc.*, **132**, 642 (1985).
8. J. A. Powell, L. G. Matus, and M. A. Kuczmarsk, *J. Electrochem. Soc.*, **134**, 1558 (1987).
9. J. D. Hwang, Y. K. Fang, Y. U. Song, and D. N. Yaung, *Jpn. J. Appl. Phys., Part 1*, **34**, 1447 (1995).
10. K. Ikoma, M. Yamanaka, H. Yamaguchi, and Y. Shich, *J. Electrochem. Soc.*, **138**, 3028 (1991).
11. H. Nagasawa, K. Yagi, and T. Kawahara, *J. Cryst. Growth*, **237–239**, 1244 (2002).
12. H. J. Kim, R. F. Davis, X. B. Cox, and R. W. Linton, *J. Electrochem. Soc.*, **134**, 2269 (1987).
13. C. C. Chiu and S. B. Desu, *J. Mater. Res.*, **8**, 535 (1993).
14. J. P. Li and A. J. Steckl, *J. Electrochem. Soc.*, **142**, 634 (1995).
15. G. Ferro, Y. Monteil, H. Vincent, V. Thevenot, M. D. Tran, F. Cauwet, and J. Bouix, *J. Appl. Phys.*, **80**, 4691 (1996).
16. A. Severino, G. D'Arrigo, C. Bongiorno, S. Scalese, F. La Via, and G. Foti, *J. Appl. Phys.*, **102**, 023518 (2007).
17. R. Scholz, U. Gösele, E. Niemann, and D. Leidich, *Appl. Phys. Lett.*, **67**, 1453 (1995).
18. R. Scholz, U. Gösele, E. Niemann, and F. Wischmeyer, *Appl. Phys. A: Mater. Sci. Process.*, **64**, 115 (1997).
19. V. Cimalla, Th. Stauden, G. Eichhorn, and J. Pezoldt, *Mater. Sci. Eng., B*, **61–62**, 553 (1999).
20. J. Yun, T. Takahashi, T. Mitani, Y. Ishida, and H. Okumura, *J. Cryst. Growth*, **291**, 148 (2006).
21. C. A. Zorman, A. J. Fleischman, A. S. Dewa, M. Mehregany, C. Jacob, S. Nishino, and P. Pirouz, *J. Appl. Phys.*, **78**, 5136 (1995).
22. W. Y. Chen, C. C. Chen, J. Hwang, and C. F. Huang, *Cryst. Growth Des.*, **9**, 2616 (2009).
23. S. Nishino, Y. Hazuki, H. Matsunami, and T. Tanaka, *J. Electrochem. Soc.*, **127**, 2674 (1980).
24. K. Yagi and H. Nagasawa, *Mater. Sci. Forum*, **264–268**, 191 (1998).

Downloaded on 2014-04-24 to IP 140.113.38.11 address. Redistribution subject to ECS terms of use (see ecsdl.org/site/terms_use) unless CC License in place (see abstract).